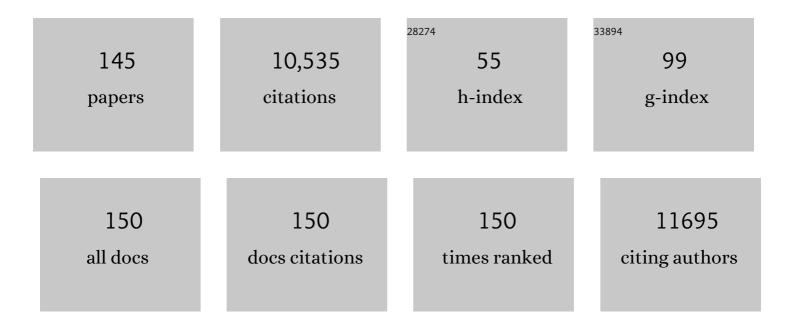
Hangrong Chen

List of Publications by Year in descending order

Source: https://exaly.com/author-pdf/7576919/publications.pdf Version: 2024-02-01



#	Article	IF	CITATIONS
1	In Vivo Bio afety Evaluations and Diagnostic/Therapeutic Applications of Chemically Designed Mesoporous Silica Nanoparticles. Advanced Materials, 2013, 25, 3144-3176.	21.0	636
2	Hollow/Rattle-Type Mesoporous Nanostructures by a Structural Difference-Based Selective Etching Strategy. ACS Nano, 2010, 4, 529-539.	14.6	615
3	A Facile Oneâ€Pot Synthesis of a Twoâ€Dimensional MoS ₂ /Bi ₂ S ₃ Composite Theranostic Nanosystem for Multiâ€Modality Tumor Imaging and Therapy. Advanced Materials, 2015, 27, 2775-2782.	21.0	385
4	Biocompatible PEGylated MoS2 nanosheets: Controllable bottom-up synthesis and highly efficient photothermal regression of tumor. Biomaterials, 2015, 39, 206-217.	11.4	304
5	Manganese oxide-based multifunctionalized mesoporous silica nanoparticles for pH-responsive MRI, ultrasonography and circumvention of MDR in cancer cells. Biomaterials, 2012, 33, 7126-7137.	11.4	278
6	"Manganese Extraction―Strategy Enables Tumor-Sensitive Biodegradability and Theranostics of Nanoparticles. Journal of the American Chemical Society, 2016, 138, 9881-9894.	13.7	246
7	Multifunctional Mesoporous Nanoellipsoids for Biological Bimodal Imaging and Magnetically Targeted Delivery of Anticancer Drugs. Advanced Functional Materials, 2011, 21, 270-278.	14.9	239
8	Injectable 2D MoS ₂ â€Integrated Drug Delivering Implant for Highly Efficient NIRâ€Triggered Synergistic Tumor Hyperthermia. Advanced Materials, 2015, 27, 7117-7122.	21.0	238
9	A Prussian Blueâ€Based Core–Shell Hollow‣tructured Mesoporous Nanoparticle as a Smart Theranostic Agent with Ultrahigh pHâ€Responsive Longitudinal Relaxivity. Advanced Materials, 2015, 27, 6382-6389.	21.0	233
10	Au capped magnetic core/mesoporous silica shell nanoparticles for combined photothermo-/chemo-therapy and multimodal imaging. Biomaterials, 2012, 33, 989-998.	11.4	230
11	Ultrasound-Triggered Nitric Oxide Release Platform Based on Energy Transformation for Targeted Inhibition of Pancreatic Tumor. ACS Nano, 2016, 10, 10816-10828.	14.6	229
12	Perfluorohexaneâ€Encapsulated Mesoporous Silica Nanocapsules as Enhancement Agents for Highly Efficient High Intensity Focused Ultrasound (HIFU). Advanced Materials, 2012, 24, 785-791.	21.0	207
13	Colloidal HPMO Nanoparticles: Silicaâ€Etching Chemistry Tailoring, Topological Transformation, and Nanoâ€Biomedical Applications. Advanced Materials, 2013, 25, 3100-3105.	21.0	205
14	Black titania-based theranostic nanoplatform for single NIR laser induced dual-modal imaging-guided PTT/PDT. Biomaterials, 2016, 84, 13-24.	11.4	189
15	Ultrasmall Cu _{2â€<i>x</i>} S Nanodots for Highly Efficient Photoacoustic Imagingâ€Guided Photothermal Therapy. Small, 2015, 11, 2275-2283.	10.0	184
16	Perfluorooctyl bromide & indocyanine green co-loaded nanoliposomes for enhanced multimodal imaging-guided phototherapy. Biomaterials, 2018, 165, 1-13.	11.4	173
17	Multifunctional Mesoporous Composite Nanocapsules for Highly Efficient MRIâ€Guided Highâ€Intensity Focused Ultrasound Cancer Surgery. Angewandte Chemie - International Edition, 2011, 50, 12505-12509.	13.8	166
18	Microbubbles from Gasâ€Generating Perfluorohexane Nanoemulsions for Targeted Temperature‧ensitive Ultrasonography and Synergistic HIFU Ablation of Tumors. Advanced Materials, 2013, 25, 4123-4130.	21.0	160

#	Article	IF	CITATIONS
19	Prussian Blue Nanozyme with Multienzyme Activity Reduces Colitis in Mice. ACS Applied Materials & Interfaces, 2018, 10, 26108-26117.	8.0	157
20	Bi 2 S 3 -embedded mesoporous silica nanoparticles for efficient drug delivery and interstitial radiotherapy sensitization. Biomaterials, 2015, 37, 447-455.	11.4	156
21	A Versatile Nanotheranostic Agent for Efficient Dualâ€Mode Imaging Guided Synergistic Chemoâ€Thermal Tumor Therapy. Advanced Functional Materials, 2015, 25, 2520-2529.	14.9	155
22	Highly Efficient 2D NIRâ€ I Photothermal Agent with Fenton Catalytic Activity for Cancer Synergistic Photothermal–Chemodynamic Therapy. Advanced Science, 2020, 7, 1902576.	11.2	153
23	Structure-property relationships in manganese oxide - mesoporous silica nanoparticles used for T1-weighted MRI and simultaneous anti-cancer drug delivery. Biomaterials, 2012, 33, 2388-2398.	11.4	135
24	Au-nanoparticle coated mesoporous silica nanocapsule-based multifunctional platform for ultrasound mediated imaging, cytoclasis and tumor ablation. Biomaterials, 2013, 34, 2057-2068.	11.4	135
25	Endogenous Catalytic Generation of O ₂ Bubbles for <i>In Situ</i> Ultrasound-Guided High Intensity Focused Ultrasound Ablation. ACS Nano, 2017, 11, 9093-9102.	14.6	133
26	A Drug–Perfluorocarbon Nanoemulsion with an Ultrathin Silica Coating for the Synergistic Effect of Chemotherapy and Ablation by Highâ€Intensity Focused Ultrasound. Advanced Materials, 2014, 26, 7378-7385.	21.0	130
27	Engineering Inorganic Nanoemulsions/Nanoliposomes by Fluorideâ€Silica Chemistry for Efficient Delivery/Coâ€Delivery of Hydrophobic Agents. Advanced Functional Materials, 2012, 22, 1586-1597.	14.9	128
28	Biodegradable Fe(III)@WS ₂ â€PVP Nanocapsules for Redox Reaction and TMEâ€Enhanced Nanocatalytic, Photothermal, and Chemotherapy. Advanced Functional Materials, 2019, 29, 1901722.	14.9	128
29	Ultrasmall mesoporous organosilica nanoparticles: Morphology modulations and redox-responsive biodegradability for tumor-specific drug delivery. Biomaterials, 2018, 161, 292-305.	11.4	127
30	Enabling Prussian Blue with Tunable Localized Surface Plasmon Resonances: Simultaneously Enhanced Dual-Mode Imaging and Tumor Photothermal Therapy. ACS Nano, 2016, 10, 11115-11126.	14.6	123
31	Clearable Theranostic Platform with a pH-Independent Chemodynamic Therapy Enhancement Strategy for Synergetic Photothermal Tumor Therapy. ACS Applied Materials & Interfaces, 2019, 11, 18133-18144.	8.0	120
32	Reversible Pore‧tructure Evolution in Hollow Silica Nanocapsules: Large Pores for siRNA Delivery and Nanoparticle Collecting. Small, 2011, 7, 2935-2944.	10.0	117
33	Multifunctional Graphene Oxideâ€based Triple Stimuliâ€Responsive Nanotheranostics. Advanced Functional Materials, 2014, 24, 4386-4396.	14.9	115
34	Engineering Singleâ€Atom Cobalt Catalysts toward Improved Electrocatalysis. Small, 2018, 14, e1704319.	10.0	97
35	Facile Synthesis of Magnetite/Perfluorocarbon Coâ€Loaded Organic/Inorganic Hybrid Vesicles for Dualâ€Modality Ultrasound/Magnetic Resonance Imaging and Imagingâ€Guided Highâ€Intensity Focused Ultrasound Ablation. Advanced Materials, 2013, 25, 2686-2692.	21.0	93
36	CO ₂ bubbling-based 'Nanobomb' System for Targetedly Suppressing Panc-1 Pancreatic Tumor via Low Intensity Ultrasound-activated Inertial Cavitation. Theranostics, 2015, 5, 1291-1302.	10.0	90

#	Article	IF	CITATIONS
37	A Multifunctional Theranostic Nanoagent for Dual-Mode Image-Guided HIFU/Chemo- Synergistic Cancer Therapy. Theranostics, 2016, 6, 404-417.	10.0	85
38	A facile synthesis of versatile Cu2â^'xS nanoprobe for enhanced MRI and infrared thermal/photoacoustic multimodal imaging. Biomaterials, 2015, 57, 12-21.	11.4	83
39	A continuous tri-phase transition effect for HIFU-mediated intravenous drug delivery. Biomaterials, 2014, 35, 5875-5885.	11.4	80
40	An Intelligent Nanotheranostic Agent for Targeting, Redoxâ€Responsive Ultrasound Imaging, and Imagingâ€Guided Highâ€Intensity Focused Ultrasound Synergistic Therapy. Small, 2014, 10, 1403-1411.	10.0	78
41	A Robust ROS Generation Strategy for Enhanced Chemodynamic/Photodynamic Therapy via H ₂ O ₂ /O ₂ Self‣upply and Ca ²⁺ Overloading. Advanced Functional Materials, 2021, 31, 2106106.	14.9	75
42	Intelligent Nanocomposites with Intrinsic Blood–Brainâ€Barrier Crossing Ability Designed for Highly Specific MR Imaging and Sonodynamic Therapy of Glioblastoma. Small, 2020, 16, e1906985.	10.0	73
43	Fe ₃ O ₄ Mesocrystals with Distinctive Magnetothermal and Nanoenzyme Activity Enabling Self-Reinforcing Synergistic Cancer Therapy. ACS Applied Materials & Interfaces, 2020, 12, 19285-19294.	8.0	73
44	Injectable Smart Phaseâ€Transformation Implants for Highly Efficient In Vivo Magneticâ€Hyperthermia Regression of Tumors. Advanced Materials, 2014, 26, 7468-7473.	21.0	72
45	Outside-in synthesis of mesoporous silica/molybdenum disulfide nanoparticles for antitumor application. Chemical Engineering Journal, 2018, 351, 157-168.	12.7	72
46	Photothermal Fenton Nanocatalysts for Synergetic Cancer Therapy in the Second Near-Infrared Window. ACS Applied Materials & Interfaces, 2020, 12, 30145-30154.	8.0	72
47	Key Singleâ€Atom Electrocatalysis in Metal—Organic Framework (MOF)â€Đerived Bifunctional Catalysts. ChemSusChem, 2018, 11, 3473-3479.	6.8	71
48	Photothermoâ€Promoted Nanocatalysis Combined with H ₂ Sâ€Mediated Respiration Inhibition for Efficient Cancer Therapy. Advanced Functional Materials, 2021, 31, 2007991.	14.9	70
49	Construction of microneedle-assisted co-delivery platform and its combining photodynamic/immunotherapy. Journal of Controlled Release, 2020, 324, 218-227.	9.9	66
50	Breaking the Redox Homeostasis: an Albuminâ€Based Multifunctional Nanoagent for GSH Depletionâ€Assisted Chemo″Chemodynamic Combination Therapy. Advanced Functional Materials, 2021, 31, 2100355.	14.9	66
51	Injectable and thermally contractible hydroxypropyl methyl cellulose/Fe3O4 for magnetic hyperthermia ablation of tumors. Biomaterials, 2017, 128, 84-93.	11.4	64
52	Drug delivery/imaging multifunctionality of mesoporous silica-based composite nanostructures. Expert Opinion on Drug Delivery, 2014, 11, 917-930.	5.0	62
53	Engineering Active Fe Sites on Nickel–Iron Layered Double Hydroxide through Component Segregation for Oxygen Evolution Reaction. ChemSusChem, 2020, 13, 811-818.	6.8	62
54	Numerical self-consistent-field method to solve the Kohn-Sham equations in confined many-electron atoms. Physical Review E, 1998, 58, 3949-3954.	2.1	61

#	Article	IF	CITATIONS
55	A facile in situ hydrophobic layer protected selective etching strategy for the synchronous synthesis/modification of hollow or rattle-type silica nanoconstructs. Journal of Materials Chemistry, 2012, 22, 12553.	6.7	53
56	Roothaan's approach to solve the Hartree-Fock equations for atoms confined by soft walls: Basis set with correct asymptotic behavior. Journal of Chemical Physics, 2015, 143, 034103.	3.0	50
57	2D nanostructures beyond graphene: preparation, biocompatibility and biodegradation behaviors. Journal of Materials Chemistry B, 2020, 8, 2974-2989.	5.8	50
58	Double-scattering/reflection in a Single Nanoparticle for Intensified Ultrasound Imaging. Scientific Reports, 2015, 5, 8766.	3.3	49
59	Dualâ€Mesoporous ZSMâ€5 Zeolite with Highly <i>b</i> â€Axisâ€Oriented Large Mesopore Channels for the Production of Benzoin Ethyl Ether. Chemistry - A European Journal, 2013, 19, 10017-10023.	3.3	48
60	Synergistic retention strategy of RGD active targeting and radiofrequency-enhanced permeability for intensified RF & chemotherapy synergistic tumor treatment. Biomaterials, 2016, 99, 34-46.	11.4	44
61	H2O2-responsive theranostic nanomedicine. Chinese Chemical Letters, 2017, 28, 1841-1850.	9.0	44
62	Cu/Mn co-loaded hierarchically porous zeolite beta: a highly efficient synergetic catalyst for soot oxidation. Journal of Materials Chemistry A, 2015, 3, 9745-9753.	10.3	43
63	Basis set effects on the Hartree–Fock description of confined many-electron atoms. Journal of Physics B: Atomic, Molecular and Optical Physics, 2012, 45, 015002.	1.5	42
64	Magnesiumâ€Engineered Silica Framework for pHâ€Accelerated Biodegradation and DNAzymeâ€Triggered Chemotherapy. Small, 2018, 14, e1800708.	10.0	41
65	Reshaping the Tumor Immune Microenvironment Based on a Lightâ€Activated Nanoplatform for Efficient Cancer Therapy. Advanced Materials, 2022, 34, e2108908.	21.0	41
66	Hyalase-Mediated Cascade Degradation of a Matrix Barrier and Immune Cell Penetration by a Photothermal Microneedle for Efficient Anticancer Therapy. ACS Applied Materials & Interfaces, 2021, 13, 26790-26799.	8.0	40
67	A pH and magnetic dual-response hydrogel for synergistic chemo-magnetic hyperthermia tumor therapy. RSC Advances, 2018, 8, 9812-9821.	3.6	39
68	Microfluidics-Assisted Surface Trifunctionalization of a Zeolitic Imidazolate Framework Nanocarrier for Targeted and Controllable Multitherapies of Tumors. ACS Applied Materials & Interfaces, 2020, 12, 45838-45849.	8.0	39
69	Nanoflower-like weak crystallization manganese oxide for efficient removal of low-concentration NO at room temperature. Journal of Materials Chemistry A, 2015, 3, 7631-7638.	10.3	37
70	Mesoporous Silica Nanoparticlesâ€Reinforced Hydrogel Scaffold together with Pinacidil Loading to Improve Stem Cell Adhesion. ChemNanoMat, 2018, 4, 631-641.	2.8	37
71	Self-assembly hollow manganese Prussian white nanocapsules attenuate Tau-related neuropathology and cognitive decline. Biomaterials, 2020, 231, 119678.	11.4	37
72	A combined "RAFT―and "Graft From―polymerization strategy for surface modification of mesoporous silica nanoparticles: towards enhanced tumor accumulation and cancer therapy efficacy. Journal of Materials Chemistry B, 2014, 2, 5828-5836.	5.8	36

#	Article	IF	CITATIONS
73	Engineering graphene oxide with ultrasmall SPIONs and smart drug release for cancer theranostics. Chemical Communications, 2019, 55, 1963-1966.	4.1	35
74	Inlaying Radiosensitizer onto the Polypeptide Shell of Drug-Loaded Ferritin for Imaging and Combinational Chemo-Radiotherapy. Theranostics, 2019, 9, 2779-2790.	10.0	35
75	Highly active MnO _x –CeO ₂ catalyst for diesel soot combustion. RSC Advances, 2017, 7, 3233-3239.	3.6	33
76	Electronâ€density delocalization in manyâ€electron atoms confined by penetrable walls: A <scp>H</scp> artree– <scp>F</scp> ock study. International Journal of Quantum Chemistry, 2018, 118, e25571.	2.0	33
77	A facile one-pot synthesis of hierarchically porous Cu(I)-ZSM-5 for radicals-involved oxidation of cyclohexane. Applied Catalysis A: General, 2013, 451, 112-119.	4.3	32
78	Template-Free Synthesis of Hollow/Porous Organosilica–Fe ₃ O ₄ Hybrid Nanocapsules toward Magnetic Resonance Imaging-Guided High-Intensity Focused Ultrasound Therapy. ACS Applied Materials & Interfaces, 2016, 8, 29986-29996.	8.0	32
79	Multi-metallic catalysts for the electroreduction of carbon dioxide: Recent advances and perspectives. Renewable and Sustainable Energy Reviews, 2022, 155, 111922.	16.4	32
80	A smart, phase transitional and injectable DOX/PLGA-Fe implant for magnetic-hyperthermia-induced synergistic tumor eradication. Acta Biomaterialia, 2016, 29, 298-306.	8.3	31
81	Synthesis and Surface Engineering of Inorganic Nanomaterials Based on Microfluidic Technology. Nanomaterials, 2020, 10, 1177.	4.1	30
82	Facile synthesis of spinel Cu _{1.5} Mn _{1.5} O ₄ microspheres with high activity for the catalytic combustion of diesel soot. RSC Advances, 2017, 7, 20451-20459.	3.6	28
83	Ultrasound-Enhanced Delivery of Doxorubicin-Loaded Nanodiamonds from Pullulan-all-trans-Retinal Nanoparticles for Effective Cancer Therapy. ACS Applied Materials & Interfaces, 2019, 11, 20341-20349.	8.0	28
84	A self-activating nanovesicle with oxygen-depleting capability for efficient hypoxia-responsive chemo-thermo cancer therapy. Biomaterials, 2021, 269, 120533.	11.4	27
85	Highly efficient light-induced hydrogen evolution from a stable Pt/CdS NPs-co-loaded hierarchically porous zeolite beta. Applied Catalysis B: Environmental, 2014, 152-153, 271-279.	20.2	24
86	Solution of the Kohnâ \in "Sham equations for many-electron atoms confined by penetrable walls. Theoretical Chemistry Accounts, 2016, 135, 1.	1.4	24
87	Nitrogenâ€Doped Carbon Vesicles with Dual Ironâ€Based Sites for Efficient Oxygen Reduction. ChemSusChem, 2017, 10, 499-505.	6.8	24
88	Tuning the Performance of Single-Atom Electrocatalysts: Support-Induced Structural Reconstruction. Chemistry of Materials, 2018, 30, 7494-7502.	6.7	24
89	Transferrin Receptorâ€Mediated Sequential Intercellular Nanoparticles Relay for Tumor Deep Penetration and Sonodynamic Therapy. Advanced Therapeutics, 2019, 2, 1800152.	3.2	24
90	Microfluidicsâ€Assisted Engineering of pH/Enzyme Dualâ€Activatable ZIF@Polymer Nanosystem for Coâ€Delivery of Proteins and Chemotherapeutics with Enhanced Deepâ€Tumor Penetration. Angewandte Chemie - International Edition, 2022, 61, .	13.8	24

#	Article	IF	CITATIONS
91	Confined nanoparticles growth within hollow mesoporous nanoreactors for highly efficient MRI-guided photodynamic therapy. Chemical Engineering Journal, 2020, 379, 122251.	12.7	23
92	Tuning selectivity of electrochemical reduction reaction of CO2 by atomically dispersed Pt into SnO2 nanoparticles. Chemical Engineering Journal, 2022, 430, 133035.	12.7	23
93	Mesoporeâ€Induced Aggregation of Cobalt Protoporphyrin for Photoacoustic Imaging and Antioxidant Protection of Stem Cells. Advanced Functional Materials, 2018, 28, 1804497.	14.9	21
94	Modeling Pressure Effects on the Electronic Properties of Ca, Sr, and Ba by the Confined Atoms Model. Advances in Quantum Chemistry, 2009, 58, 1-12.	0.8	21
95	Self-cycling redox nanoplatform in synergy with mild magnetothermal and autophagy inhibition for efficient cancer therapy. Nano Today, 2022, 43, 101374.	11.9	21
96	A novel mesostructured alumina–ceria–zirconia tri-component nanocomposite with high thermal stability and its three-way catalysis. Microporous and Mesoporous Materials, 2011, 143, 368-374.	4.4	20
97	Facile synthesis of liposome/Cu2â~'x S-based nanocomposite for multimodal imaging and photothermal therapy. Science China Materials, 2015, 58, 294-301.	6.3	19
98	Marriage Strategy of Structure and Composition Designs for Intensifying Ultrasound & MR & CT Trimodal Contrast Imaging. ACS Applied Materials & Interfaces, 2015, 7, 18590-18599.	8.0	19
99	Fabrication of a mesoporous Ba _{0.5} Sr _{0.5} Co _{0.8} Fe _{0.2} O _{3â^î} perovskite as a low-cost and efficient catalyst for oxygen reduction. Dalton Transactions, 2017, 46, 13903-13911.	3.3	18
100	Targeted Therapeutic-Immunomodulatory Nanoplatform Based on Noncrystalline Selenium. ACS Applied Materials & Interfaces, 2019, 11, 45404-45415.	8.0	18
101	Rational Construction of Light-Driven Catalysts for CO ₂ Reduction. Energy & Fuels, 2021, 35, 5696-5715.	5.1	18
102	Preparation of Er3+/Yb3+ co-doped zeolite-derived silica glass and its upconversion luminescence property. Ceramics International, 2013, 39, 8865-8868.	4.8	17
103	A Bioenvironment-Responsive Versatile Nanoplatform Enabling Rapid Clearance and Effective Tumor Homing for Oxygen-Enhanced Radiotherapy. Chemistry of Materials, 2018, 30, 5412-5421.	6.7	17
104	Na+-induced in situ reconstitution of metal phosphate enabling efficient electrochemical water oxidation in neutral and alkaline media. Chemical Engineering Journal, 2020, 398, 125537.	12.7	17
105	MOFâ€Derived Cu/Bi Biâ€metallic Catalyst to Enhance Selectivity Toward Formate for CO ₂ Electroreduction. ChemElectroChem, 2022, 9, .	3.4	17
106	Hierarchically Porous SnO ₂ Coupled Organic Carbon for CO ₂ Electroreduction. ChemSusChem, 2020, 13, 5896-5900.	6.8	16
107	Surface Stability and Morphology of Calcium Phosphate Tuned by pH Values and Lactic Acid Additives: Theoretical and Experimental Study. ACS Applied Materials & Interfaces, 2022, 14, 4836-4851.	8.0	16
108	Proteinâ€based nanoplatforms for tumor imaging and therapy. Wiley Interdisciplinary Reviews: Nanomedicine and Nanobiotechnology, 2020, 12, e1616.	6.1	15

#	Article	IF	CITATIONS
109	Effect of Potassium Nitrate Modification on the Performance of Copperâ€Manganese Oxide Catalyst for Enhanced Soot Combustion. ChemCatChem, 2018, 10, 1455-1463.	3.7	14
110	On-Demand Detaching Nanosystem for the Spatiotemporal Control of Cancer Theranostics. ACS Applied Materials & Interfaces, 2019, 11, 16285-16295.	8.0	14
111	Sodium carbonate-assisted synthesis of hierarchically porous single-crystalline nanosized zeolites. Science Bulletin, 2017, 62, 1018-1024.	9.0	13
112	Multifaceted application of nanoparticle-based labeling strategies for stem cell therapy. Nano Today, 2020, 34, 100897.	11.9	13
113	One-pot synthesis of mesoporous CuOx/CeO2 co-loaded ZrO2–TiO2 nanocomposites via surfactant-free solvothermal method for catalytic removal of soot under NO/O2. Catalysis Communications, 2013, 35, 105-109.	3.3	12
114	A highly dispersed mesoporous zeolite@TiO2 – supported Pt for enhanced sulfur-resistance catalytic CO oxidation. Catalysis Communications, 2020, 142, 106042.	3.3	12
115	A self-assembled metal-polyphenolic nanomedicine for mild photothermal-potentiated chemodynamic therapy of tumors. Applied Materials Today, 2021, 25, 101235.	4.3	12
116	Eutectic molten salt assisted synthesis of highly defective and flexible ruthenium oxide for efficient overall water splitting. Chemical Engineering Journal, 2021, 425, 131707.	12.7	11
117	Construction of Heterostructured Sn/TiO ₂ /Si Photocathode for Efficient Photoelectrochemical CO ₂ Reduction. ChemSusChem, 2022, 15, .	6.8	11
118	One Step Template-Free Synthesis of Mesoporous MnOx/CeO2 Nanocomposite Oxides with Enhanced Low Temperature Catalytic Activity for CO and Hydrocarbon Oxidation. Catalysis Letters, 2016, 146, 1355-1360.	2.6	10
119	Low Pt‣oaded Mesoporous Sodium Germanate as a Highâ€Performance Electrocatalyst for the Oxygen Reduction Reaction. ChemSusChem, 2016, 9, 2337-2342.	6.8	10
120	Synthesis and performance of high efficient diesel oxidation catalyst based on active metal species-modified porous zeolite BEA. Journal of Catalysis, 2019, 379, 138-146.	6.2	10
121	Electron Density Analysis for the H2+ System Confined by Hard Walls: The Chemical Bond Under Extreme Conditions. Annalen Der Physik, 2019, 531, 1800476.	2.4	10
122	A Bismuth Species-Decorated ZnO/p-Si Photocathode for High Selectivity of Formate in CO ₂ Photoelectrochemical Reduction. ACS Sustainable Chemistry and Engineering, 2022, 10, 2380-2387.	6.7	10
123	Pt/Fe co-loaded mesoporous zeolite beta for CO oxidation with high catalytic activity and water resistance. RSC Advances, 2019, 9, 28089-28094.	3.6	9
124	Design strategy of optical probes for tumor hypoxia imaging. Science China Life Sciences, 2020, 63, 1786-1797.	4.9	9
125	Nanomedicine: Break-up of Two-Dimensional MnO2Nanosheets Promotes Ultrasensitive pH-Triggered Theranostics of Cancer (Adv. Mater. 41/2014). Advanced Materials, 2014, 26, 7018-7018.	21.0	8
126	Boosting neutral hydrogen evolution reaction on iridium by support effect of W18O49. Applied Catalysis A: General, 2021, 623, 118293.	4.3	8

#	Article	IF	CITATIONS
127	Nanosized Hollow Colloidal Organosilica Nanospheres with High Elasticity for Contrast-Enhanced Ultrasonography of Tumors. ACS Biomaterials Science and Engineering, 2018, 4, 248-256.	5.2	7
128	A metal protoporphyrin-induced nano-self-assembly for potentiating photothermal therapy by depleting antioxidant defense systems. Chemical Engineering Journal, 2021, 420, 129769.	12.7	7
129	TiO ₂ and Cu _{1.5} Mn _{1.5} O ₄ co-modified hierarchically porous zeolite Beta for soot oxidation with excellent sulfur-resistance and stability. Dalton Transactions, 2017, 46, 6111-6116.	3.3	6
130	Nanoflower-like Mg-doped MnOx for facile removal of low-concentration NOx at room temperature. Catalysis Communications, 2017, 97, 70-73.	3.3	6
131	Probing Nitrogenâ€Doping Effects in the Coreâ€Shell Structured Catalysts for Bifunctional Electrocatalysis ChemCatChem, 2018, 10, 4248-4252.	3.7	6
132	Recent deveolpment of multifunctional responsive gas-releasing nanoplatforms for tumor therapeutic application. Nano Research, 2023, 16, 3924-3938.	10.4	6
133	Symmetry-breaking assembled porous calcite microspheres and their multiple dental applications. Science China Materials, 2017, 60, 516-528.	6.3	5
134	Hypoxia-Induced Photogenic Radicals by Eosin Y for Efficient Phototherapy of Hypoxic Tumors. ACS Applied Bio Materials, 2020, 3, 8962-8969.	4.6	5
135	Stepwise drug release from a nanoplatform under MR-assisted focused ultrasound stimulation. Chemical Engineering Journal, 2021, 417, 128004.	12.7	4
136	Microfluidicsâ€Assisted Engineering of pH/Enzyme Dualâ€Activatable ZIF@Polymer Nanosystem for Coâ€Delivery of Proteins and Chemotherapeutics with Enhanced Deepâ€Tumor Penetration. Angewandte Chemie, 0, , .	2.0	4
137	A NTR and O2 programmed responsive photogenic radicals for efficient hypoxia cancer therapy. Sensors and Actuators B: Chemical, 2022, 369, 132311.	7.8	4
138	Disulfide Bond Reversible Strategy Enables GSH Responsiveâ€Transferrin Nanoparticles for Precise Chemotherapy. Advanced Therapeutics, 2020, 3, 2000064.	3.2	3
139	A cation exchange strategy to construct a targeting nanoprobe for enhanced <i>T</i> ₁ -weighted MR imaging of tumors. Journal of Materials Chemistry B, 2020, 8, 8519-8526.	5.8	3
140	One pot synthesis of mesostructured non-silica oxides nanocrystallites. Journal of Materials Science, 2009, 44, 6531-6537.	3.7	2
141	Nanoparticles: Colloidal HPMO Nanoparticles: Silicaâ€Etching Chemistry Tailoring, Topological Transformation, and Nanoâ€Biomedical Applications (Adv. Mater. 22/2013). Advanced Materials, 2013, 25, 3136-3136.	21.0	2
142	La2O2CO3-Induced phase composition oscillation in La–Cu mixed oxides during repeated catalytic soot combustion. Catalysis Science and Technology, 2019, 9, 5100-5110.	4.1	2
143	Efficient electrocatalytic CO2 conversion into formate with AlxBiyOz nanorods in a wide potential window. Catalysis Science and Technology, 0, , .	4.1	2
144	Simultaneous Al ₂ O ₃ Doping and Sulfation in Hierarchically Porous ZrO ₂ Solid Acids by an Oneâ€pot Synthesis for Enhanced Recycling Catalytic Performances. Chinese Journal of Chemistry, 2011, 29, 483-488.	4.9	1

#	Article	IF	CITATIONS
145	Facile synthesis and large third-order optical nonlinearity of Manganese-loaded mesoporous silica thin films. Materials Letters, 2010, 64, 1626-1629.	2.6	Ο